# FT-IR study of Cu substituted Ni-Zn ferrites prepared by citrate precursor method

**Biju Thangjam[1,2]*, Ibetombi Soibam[2]**

[1]*Physics Department, D. M. College of Science, Manipur University, Imphal, 795001, India*
[2]*Department of Physics, NIT Manipur, Langol, Imphal, 795004, India*

*Corresponding author, E-mail: bijuthdmc@gmail.com; Tel: (+91)98-56085407, (+91)98-56093533

**Received: 30 March 2016, Revised: 29 September 2016 and Accepted: 03 August 2016**

DOI: 10.5185/amp.2017/3014
www.vbripress.com/amp

## Abstract

Ni-Cu-Zn ferrites with compositional formula $Ni_{0.8-x}Cu_xZn_{0.2}Fe_2O_4$, where $0.0 \leq x \leq 0.5$ in steps of 0.1 were synthesized by the citrate precursor method. The samples were subjected to final sintering at 900°C for 2h after a pre-sintering at 600°C for 4h. X-ray diffraction patterns confirmed the formation of single phase spinel structure. The average crystallite size was calculated using Scherrer's formula and was found to vary from 33nm to 39nm, clearly indicating the formation of nanoparticles. The infrared spectra were recorded at room temperature for all the samples in the range of 450 $cm^{-1}$ to 4000 $cm^{-1}$ using Perkin Elmer FT-IR Spectrometer. Jahn-Teller effect emerges which can be identified through the FT-IR Spectroscopy of the samples. This phenomenon may result in useful electro and magneto- optical applications. Possible mechanism is being discussed. Copyright © 2017 VBRI Press.

**Keywords:** Ferrites, citrate precursor method, FT-IR, force constants, Jahn-Teller effect.

## Introduction

Nanostructured spinel type ferrites are promising materials for magneto-sensor, thermal medicine, micro-electro mechanical system, bio-sensor, magneto- electronics, data-storage media, computer hard disks, microwave electronic devices and nanotransistors [**1**]. Among the nanospinel ferrites, Ni-Zn ferrite, is becoming a technologically important material due to its high permeability, high resistivity, low eddy current losses, reasonable cost, chemical stability etc. [**2**,**3**]. It is found to be used as a magnetic material of multilayer chip inductors (MLCIs) which are important components in notebooks, cellular phones etc. The internal electrode material of MLCIs is usually Ag but prevention of Ag diffusion into the ferrite is required. This is possible if the sintering temperature of the ferrite samples is below 961°C [**4**]. There are many ways to lower the sintering temperature and substitution of $Cu^{2+}$ is one of such kind. It is also found that $Cu^{2+}$ gives more densification and improves the electromagnetic properties. Moreover, it is reported that the addition of $Cu^{2+}$ results in structural phase transition and reduction in crystal symmetry due to co-operative Jahn-Teller effect which gives rise to interesting electrical, magnetic and optical properties [**3**,**5**].

Therefore, in the present work, the structural effect of $Cu^{2+}$ substitution on NiZn ferrite synthesized by Citrate Precursor method is being investigated. The FT-IR spectra can be used for determining the local symmetry and the ordering in ferrites. It has been reported that many $Cu^{2+}$ salts and complexes exhibit tetragonally distorted octahedral structures [**6].** Hence, a discussion of Jahn- Teller effect [**7**] is given and the occurrence of lattice distortion resulting from the occupancy of lattice sites by $Cu^{2+}$ ions is being studied using FT-IR technique.

## Experimental

### *Materials*

The materials used were nickel nitrate $Ni(NO_3)_2.6H_2O$, 98% (Merck, India), copper nitrate $Cu(NO_3)_2.3H_2O$, 99% (Merck, India), zinc nitrate $Zn(NO_3)_2.6H_2O$, 96.003% (Merck, India), ferric nitrate $Fe(NO_3)_3.9H_2O$, 98% (Merck, India) and citric acid $C_6H_8O_7$, 99% (Merck, India).

### *Materials synthesis*

Appropriate amounts of nitrates and citric acid were dissolved to form a solution. The molar ratio of nitrates to citric acid was 1:1. A small amount of ammonia was added to the solution to control the pH value at 7. The solution was heated at 40°C for 30min with continuous stirring to obtain a homogeneous solution. This solution was heated at 100°C to form a viscous gel. Finally, the gel ignited in a self-propagating manner giving the ferrite powder.

The ferrite powder so obtained was pressed into pellets using 10 wt.% polyvinyl alcohol as a binder. All the samples were given final sintering at 900°C for 2h after a pre-sintering at 600°C for 4h in a programmable conventional furnace. The schematic of the chemical reaction is shown in **Fig. 1** [**8**].

The general nitrate-citrate combustion reaction may be written as follows:

$$(0.8\text{-}x)Ni(NO_3)_2.6H_2O + xCu(NO_3)_2.3H_2O + 0.2\,Zn(NO_3)_2.6H_2O + 2Fe(NO_3)_3.9H_2O + 3C_6H_8O_7 \xrightarrow{NH_3}$$

$$Ni_{0.8-x}Cu_xZn_{0.2}Fe_2O_4 + 4N_2\uparrow + 18C0_2\uparrow + 36H_20\uparrow + \text{Other products}$$

### *Characterizations*

The phase identification and structure analysis of the sintered samples were performed using X-Pert Pro PANalytical X-ray diffractometer with Cu Kα radiation. The Fourier transform infrared (FTIR) spectrum was taken in the range of 450 $cm^{-1}$ to 4000 $cm^{-1}$ using FT-IR spectrophotometer (model Perkin Elmer Spectrum two).

## Results and discussion

### *X-ray diffraction*

The X-ray diffraction (XRD) patterns of Cu substituted NiZn ferrites showed the formation of spinel cubic structure with the Fd-3m space group, which is consistent with the powder diffraction file of JCPDS card no. 01-071-3850. The patterns showed the absence of other impurity phase.

The variation of lattice parameter 'a', theoretical density '$d_x$' and experimental density '$d_e$' as a function of $Cu^{2+}$ ion concentration is given in **Table 1**.

Lattice parameter has been calculated using the formula,

$$a = d(h^2+k^2+l^2)^{1/2}$$

where, d = interplanar spacing, (hkl) = Miller indices. According to Vegard's law, lattice expansion takes place if the doping ion has larger radii than the displaced ion.

**Table 1.** Lattice parameter, density (theoretical and experimental) and crystallite size of $Ni_{0.8-x}Cu_xZn_{0.2}Fe_2O_4$.

| | Lattice parameter 'a' (Å) | Theo. density '$d_x$' ($gm/cm^3$) | Expt. Density '$d_e$' ($gm/cm^3$) | Crystallite size (nm) |
|---|---|---|---|---|
| 0.0 | 8.329 | 5.42 | 2.31 | 39.3 |
| 0.1 | 8.330 | 5.43 | 2.52 | 33.1 |
| 0.2 | 8.330 | 5.44 | 3.15 | 37.8 |
| 0.3 | 8.331 | 5.45 | 3.24 | 37.7 |
| 0.4 | 8.331 | 5.46 | 3.85 | 36.8 |
| 0.5 | 8.363 | 5.41 | 3.72 | 36.8 |

In the present series of ferrite samples, $Cu^{2+}$ ions of greater ionic radius 0.72 Å substitute $Ni^{2+}$ ions of smaller ionic radius 0.69 Å and lattice parameter is expected to increase. However, it is not observed and this may be due to the fact that contribution to lattice parameter does not solely depend on ionic radii but also on other interaction phenomenon, which needs further investigation [**9, 10**].

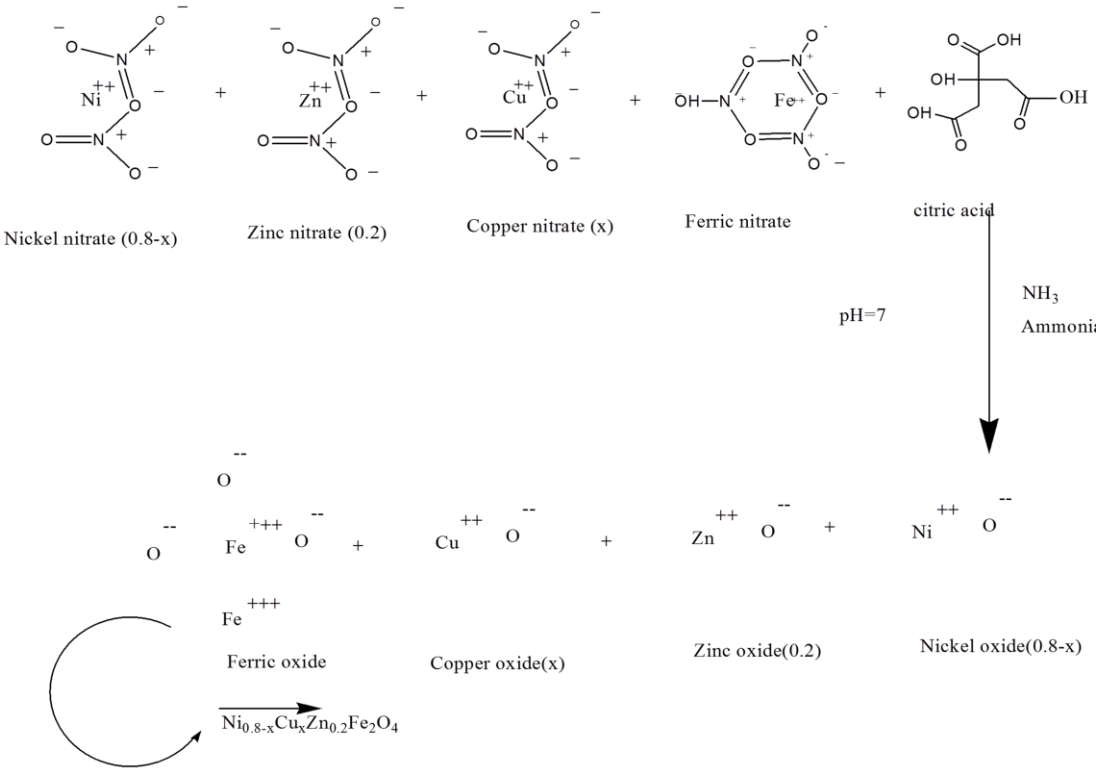


**Fig. 1.** Chemical reaction of $Ni_{0.8-x}Cu_xZn_{0.2}Fe_2O_4$.

 

Theoretical density (X-ray density) was calculated using the formula,

$d_x = 8M/Na^3$

where, M = molecular weight of the sample, N = Avogadro's number, a = lattice parameter of the sample.

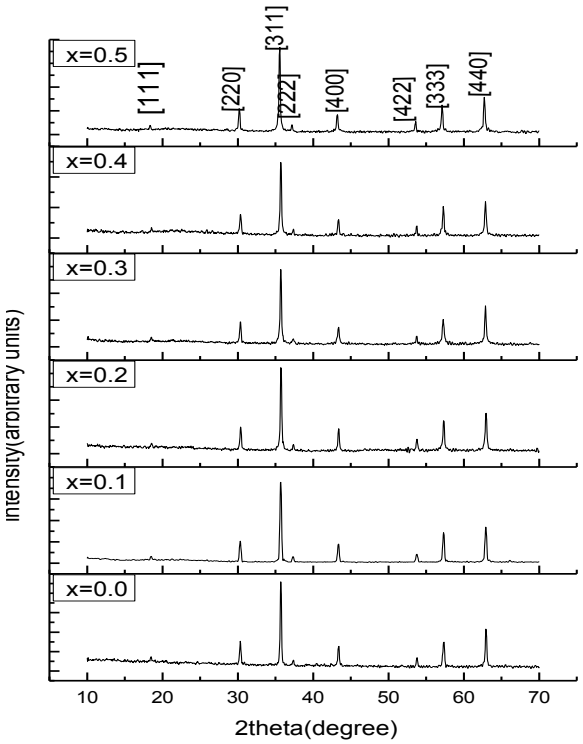


**Fig. 2.** XRD patterns of $Ni_{0.8-x}Cu_xZn_{0.2}Fe_2O_4$.

Experimental density was found out from the relation,

$d_e = W/V$

where, W = weight of the sample, V = volume of the sample. **Table 1** shows an increasing trend in density (theoretical and experimental) with increase in $Cu^{2+}$ ion concentration. This can be attributed to the fact that atomic weight of $Cu^{2+}$ (63.55 amu) is greater than that of $Ni^{2+}$ (58.71 amu). The decrease in density for the highest concentration 0.5 of the $Cu^{2+}$ ion may be accounted by the intergranular/intragranular porosity arising from discontinuous grain growth [**9**]. However, theoretical densities are larger compared to the corresponding experimental densities. This might have resulted due to the presence of pores in the samples [**9**]

The crystallite size was estimated using Debye Scherrer's formula,

$D = K\lambda/\beta\cos\theta$

where, the constant K is taken as 0.9, λ is the wavelength of X-ray used and β is the full width at half maximum of the diffraction at 2θ. The average crystallite sizes of all samples are found to be in the range of 33-39nm (**Table 1**).

### *FT-IR spectroscopy*

FT-IR absorption spectra for the sample $Ni_{0.8-x}Cu_xZn_{0.2}Fe_2O_4$ under investigation is shown in **Fig. 3**.

These spectra show two strong absorption bands at wavenumbers of about $600cm^{-1}(\bar{\upsilon}_1)$ and $450cm^{-1}(\bar{\upsilon}_2)$ for all compositions, which indicate the formation of single- phase spinel structure. These two bands can be attributed to the stretching vibrations of the tetrahedral and octahedral metal – oxygen bonds respectively in the lattices of the synthesized samples. The difference in the frequency of the two vibrations might have resulted due to the longer bond length of oxygen – metal ions in the octahedral sites and shorter bond length of oxygen – metal ions in the tetrahedral sites [**11**].

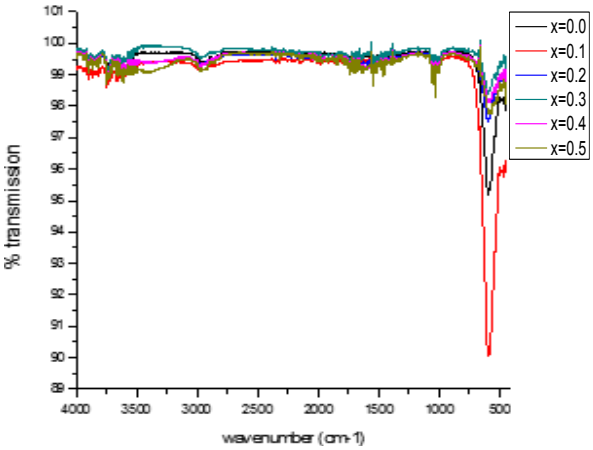


**Fig. 3.** FT-IR spectra of $Ni_{0.8-x}Cu_xZn_{0.2}Fe_2O_4$.

Owing to their larger radius and greater atomic weight, the addition of $Cu^{2+}$ ions in the octahedral sites makes the $Fe^{3+}$ ions migrate to the tetrahedral sites resulting in increase of tetrahedral vibration frequency and a decrease of the octahedral vibration frequency [**12**]. Similarly, addition of $Cu^{2+}$ ions in the tetrahedral sites results in lowering of the tetrahedral vibration frequency and increase in the octahedral vibration frequency. The subsequent changes in both the vibrational frequencies indicate that $Cu^{2+}$ ions go into both the lattice sites. The force constants for tetrahedral ($K_t$) and octahedral ($K_o$) have been calculated using the relation [**13**],

$K = 4\pi^2c^2\bar{\upsilon}^2\mu$

where, c = speed of light, $\bar{\upsilon}$ = band wave number in $cm^{-1}$, μ = reduced mass of $Fe^{3+}$ ions and $O^{2-}$ ions ($2.061 \times 10^{-23}$g). The positions of absorption bands in terms of wave number $\bar{\upsilon}_1$ (tetrahedral site) and $\bar{\upsilon}_2$(octahedral site) along with their respective force constants ($K_t$ and $K_o$) are listed in **Table 2**.

 

**Table 2.** Absorption band positions and their respective force constants.

| Conc. of the $Cu^{2+}$ ions | A site (tetrahedral | | B site ( octahedral ) | | | |
|---|---|---|---|---|---|---|
| | Wave no. $\bar{\upsilon}_1 cm^{-1}$ | Force const. $K_t$ x $10^5$ (dyne $cm^{-1}$) | Wave no. $\bar{\upsilon}_2$ ($cm^{-1}$) | Wave no. $\bar{\upsilon}_2'$ ($cm^{-1}$) | Force const. $K_o$ x $10^5$ (dyne $cm^{-1}$) | Force const. $K_o'$ x $10^5$ (dyne $cm^{-1}$) |
| 0.0 | 600 | 2.63 | 453 | --- | 1.50 | --- |
| 0.1 | 592 | 2.56 | 455 | --- | 1.51 | --- |
| 0.2 | 601 | 2.64 | 452 | --- | 1.49 | --- |
| 0.3 | 601 | 2.64 | 452 | --- | 1.49 | --- |
| 0.4 | 592 | 2.56 | 453 | 459 | 1.50 | 1.54 |
| 0.5 | 592 | 2.56 | 453 | 457 | 1.50 | 1.53 |

These force constants are in agreement with the elastic and thermodynamic properties of these compounds and are sensitive to the distribution of metal ions between the alternate sites [**14**]. The observed change in wave numbers and force constants with the change in $Cu^{2+}$ concentration shows that $Cu^{2+}$ ions occupy both the A and B sites.

There is a weak splitting around octahedral vibration frequency ($\upsilon_2'$) which can be accounted by the existence of $Cu^{2+}$ ions, a Jahn-Teller ion [**12**] in the octahedral sites. This results in some lattice distortion, which is explained as follows:

In an electronically degenerate state, the degenerate orbitals are occupied in an asymmetrical manner, thereby resulting in more energy. The system, therefore, manages to lower the energy by lowering the overall symmetry of the molecule i.e. by undergoing distortion, which is known as Jahn-Teller distortion. It is known that $Cu^{2+}$ ion has $d^9$ configuration and its octahedral arrangement results in crystal field splitting of the d orbitals into lower energy $t_{2g}$ and higher energy $e_g$ levels so that the electrons are arranged as follows:

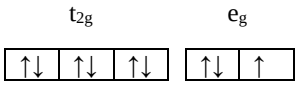


The three $e_g$ electrons occupy the $d_{x^2-y^2}$ and $d_{z^2}$ orbitals making the $e_g$ level asymmetrically occupied and thereby favors Jahn-Teller distortion. The degeneracy of the $e_g$ and $t_{2g}$ orbitals are removed and the complex gets distorted. The $d_{x^2-y^2}$ orbital is under the effect of four ligands approaching along the directions +x, -x, +y and –y while the $d_{z^2}$ orbital is under the effect of only two ligands approaching along the directions +z and –z. Hence, the energy of the $d_{x^2-y^2}$ orbital becomes greater than that of the $d_{z^2}$ orbital. As a result, the three electrons in the $e_g$ level are arranged as: $(d_{z^2})^2$ $(d_{x^2-y^2})^1$. Now, since the $d_{z^2}$ orbital contains two electrons, the ligands approaching along the +z and –z directions are restricted from coming close to the $Cu^{2+}$ ion as those approaching along +x, -x, +y and –y [**6**]. The octahedral arrangement therefore gets distorted and there is a splitting observed around the octahedral vibrational frequency ($\upsilon_2'$).

## Conclusion

The XRD patterns and FT-IR spectra of the samples confirm the cubic spinel structure of the synthesized ferrites. The observed crystallite size of the ferrite samples ranged from 33 nm to 39 nm, indicating that ferrite nanocrystals can be synthesized by the Citrate Precursor Method. The alteration in the absorption frequency bands of the FT-IR spectrum indicates the change in the $Fe^{3+}$ - $O^{2-}$ inter nuclear distances for the tetrahedral and octahedral sites respectively. The splitting of the vibrational frequencies of the lattice sites can be accounted by the existence of $Cu^{2+}$ ion, a Jahn-Teller ion which causes some lattice distortion. However, an in-depth study is needed to be carried out, so that, it may give the possibility for electro and magneto-optical applications.

### Acknowledgements

The authors would like to acknowledge Manipur University for the XRD measurements and Dr. Thiyam David Singh, Assistant Professor (Chemistry), NIT Manipur for the FT-IR measurements.

### References

1. Bayrakdar, H.; Yalcin, O.; Vural, S.; Esmer, K.; *J. Magn. Magn. Mater*., **2013**, *343*, 86. **DOI:** 10.1016/j.jmmm.2013.04.079
2. Jahanbin, T.; Hasim, M.; Mantori, K. A.; *J. Magn. Magn. Mater*., **2010**, *322*, 2684. **DOI:** 10.1016/j.jmmm.2010.04.008
3. Jadhav, P. A.; Devan, R. S.; Kolekar, Y. D.; Chougule, B. K.; *J. Phys. Chem. Solids*, **2009**,*70*, 396. **DOI:** 10.1016/j.jpcs.2008.11.019
4. Dimri, M. C.; Verma, A.; Kashyap, S. C.; Dube, D.C.; Thakur, O. P.; Prakash, C.; *Mater. Sci. Eng., B*, **2006**, *133*, 42. **DOI:** 10.1016/j.mseb.2006.04.043
5. Huq, M. F.; Saha, D. K.; Ahmed, R.; Mahmood, Z. H.; *J. Sci. Res*., **2013**, *5*, 215. **DOI:** 10.3329/jsr.v5i212434
6. Lee, J. D. (Eds.); Concise Inorganic Chemistry; Wiley: UK, **1996**. **ISBN:** 978-81-265-1554-7
7. Koppel, H.; Yarkony, D. R.; Barentzen, H. (Eds.); The Jahn-Teller Effect: Fundamentals and Implications for Physics and Chemistry; Springer Science & Business Media: Germany, **2009**. **DOI:** 10.1007/978-3-642-03432-9
8. Awati, V. V.; Rathod, S. M.; Mane, M. L.; Mohite, K.C.; *Int. Nano Lett*., **2013**, *3*, 2. **DOI:** 10.1186/2228-5326-3-29
9. Hossain, A. A.; Rahman, M. L.; *J. Magn. Magn. Mater*., **2011**, *323*, 1956. **DOI:** 10.1016/j.jmmm.2011.02.031
10. Soibam, I.; Phanjoubam, S.; Prakash, C.; *J. Magn. Magn. Mater*., **2009**, *321*, 2780. **DOI:** 10.1016/j.jmmm.2009.04.011
11. Raju, M. K.; *Chem. Sci. Trans*., **2015**, *4*, 138. **DOI:** 10.7598/cst2015.957
12. Tehrani, F. S.; Daadmehr, V.; Rezakhani, A. T.; Akbarnejad, R. H.; Gholipour, S.; *J. Supercond. Novel Magn*., **2012**, *25*, 2449. **DOI:** 10.1007/s10948-012-1655-5
13. Pavia, D. L.; Lampman, G. M.; Kriz, G. S. (Eds.); Introduction to Spectroscopy; Cengage Learning: USA, **2001**. **ISBN:** 0-03-031961-7
14. Waldron, R. D.; *Phys. Rev*., **1955**, *99*, 1727. **DOI:** 10.1103/PhysRev.99.1727

 